

- P. R. Sager, P. A. Brown, R. D. Berlin, *Cell* **39**, 275 (1984).
51. J. Trifaro and N. Kenigsberg, *Fed. Proc. Fed. Am. Soc. Exp. Biol.* **42**, 961 (1983); R. A. Steinhardt and J. M. Alderton, *Nature (London)* **295**, 154 (1982).
52. J. E. Hooper and R. B. Kelly, *J. Biol. Chem.* **259**, 148 (1984); *ibid.*, p. 141; R. D. Burgoyne and M. J. Gelson, *FEBS Lett.* **131**, 127 (1981); S. Grinstein and W. Furaya, *ibid.* **140**, 49 (1982); S. F. Olsen, J. Slaninova, M. Trieman, T. Saemark, N. A. Thorn, *Acta Physiol. Scand.* **118**, 355 (1983); N. Moskowitz, W. Schook, K. Beckenstein, S. Puzskin, *Brain Res.* **263**, 243 (1983).
53. E. Vila-Porcile and L. Oliver, in *Synthesis and Release of Adenohypophyseal Hormones*, M. Jutisz and K. W. McKerns, Eds. (Plenum, New York, 1980), pp. 67-103; W. D. Matthews, L. Tsavaler, L. F. Reichardt, *J. Cell Biol.* **91**, 257 (1981); K. Kawai, I. Ipp, L. Orci, A. Perellet, R. H. Unger, *Science* **218**, 447 (1982).
54. S. P. Gilbert and R. D. Sloboda, *J. Cell Biol.* **99**, 445 (1984); S. T. Brady, R. J. Lasek, R. D. Allen, *Science* **218**, 1129 (1982); R. D. Vale, B. J. Schnapp, T. S. Reese, M. P. Sheetz, *Cell*, in press; T. Schroer, S. Brady, R. B. Kelly, *J. Cell Biol.* **101**, 568 (1985).
55. R. N. Melmed, C. Beniter, S. J. Holt, *J. Cell Sci.* **11**, 449 (1972).
56. R. B. Kelly et al., *Cold Spring Harbor Symp. Quant. Biol.* **47**, 697 (1984); J. M. Trifaro and R. W. H. Lee, *Neuroscience* **5**, 1533 (1980).
57. F. Malaisse-Lagae, M. Amherdt, M. Ravazzola, A. Sener, J. C. Hutton, L. Orci, W. J. Malaisse, *J. Clin. Invest.* **63**, 1284 (1979); S. L. Howell, M. Tyhurst, *Cell Tissue Res.* **190**, 163 (1978); J. A. Williams, *Methods Cell Biol.* **23**, 247 (1981).
58. C. M. Redman, D. Banerjee, S. Yu, *Methods Cell Biol.* **23**, 231 (1981); G. Bennett, S. Parsons, E. Carlet, *Am. J. Anat.* **170**, 521 (1984).
59. G. Bennett, E. Carlet, G. Wild, S. Parsons, *Am. J. Anat.* **170**, 545 (1984); J. Blok, L. A. Ginsel, A. A. Mulder-Stapel, J. J. M. Onderwater, W. Th. Daems, *Cell Tissue Res.* **215**, 1 (1981); A. Quaroni, K. Kirsch, M. M. Weiser, *Biochem. J.* **182**, 213 (1979).
60. E. P. Reaven and G. M. Reaven, *J. Cell Biol.* **75**, 559 (1977).
61. A. A. Rogalski, J. E. Bergmann, S. J. Singer, *ibid.* **99**, 1101 (1984).
62. Although studies have been made on the effects of colchicine on bone marrow-derived secretory cells, the results cannot readily be compared to those on other regulated secretory cells. Since platelets and neutrophils and resting mast cells synthesize little, if any, of their secretory products, it is difficult to look at the fate of newly synthesized material. Secondly, in platelets and neutrophils, secretory vesicles do not fuse with plasma membrane at the periphery; they release their contents on stimulation into internal membranes. There is no need therefore for directed transport to the cell surface [J. G. White, in *Cell Biology of the Secretory Process*, M. Cantin, Ed. (Karger, Basel, 1984), pp. 546-569; J. E. Smolen, H. M. Korchak, G. Weissmann, in *ibid.*, pp. 517-545; T. W. Martin and D. Lagunoff, in *ibid.*, pp. 481-516].
63. M. G. Farquhar and G. E. Palade, *J. Cell Biol.* **91**, 77s (1981).
64. The author expresses his deepest gratitude to members of his laboratory in discussion with whom the ideas presented here have arisen, evolved and matured. The contributions and comments of Drs. Daniel Cutler, Barry Gumbiner, Suzanne Pfeffer, Ira Mellman, Stuart Kornfeld, Peter Walter, and Jack Rose are also gratefully acknowledged. And, once again, Leslie Spector outdid herself in patience and precision while putting together the many drafts of this article.

RESEARCH ARTICLE

Structure of the GDP Domain of EF-Tu and Location of the Amino Acids Homologous to *ras* Oncogene Proteins

Frances Journak

During protein biosynthesis in *Escherichia coli*, the elongation factor (EF-)Tu recognizes, transports, and positions the codon-specified aminoacyl-transfer RNA onto the A site of the ribosome (1). In this role, EF-Tu interacts with several cellular components, including guanosine diphosphate (GDP) and guanosine triphosphate (GTP), which act as allosteric effectors to control the protein conformation required during the elongation cycle.

In comparison to adenosine-binding proteins, there are relatively few proteins that bind to guanosine, with EF-Tu being the most widely characterized. It was, therefore, of considerable interest when a family of *ras* oncogene proteins, termed p21, were found to be GDP- and GTP-binding proteins (2). In subsequent comparisons of the amino acid sequence of EF-Tu with the human Harvey C-H *ras* 1 gene product (*H-ras*) as well as with other known GDP-binding proteins (4, 5), four principal regions of homology were identified if conserved amino acid substitutions are included. In addition, several invariant amino acids were identified in all GDP-binding proteins that

have been sequenced (4). I now present my biochemical and preliminary high-resolution crystallographic results on a trypsin-modified form of EF-Tu-GDP. The locations of the amino acid sequence homology between EF-Tu and the *H-ras* p21 protein are described.

EF-Tu-GDP was isolated from *Escherichia coli* B cells and treated with TPCK-trypsin (TPCK, tosylamidophenylethyl chloromethyl ketone) (6). In all preparations, the protein was routinely passed over a G-100 Sephadex column after the trypsin digestion. A minor peak, trailing the major peak identified as trypsin-modified EF-Tu, was routinely detected by absorbance at 238 nm. In the original preparation, the minor peak was isolated and sequenced (7). The minor peak contained a 14-amino-acid peptide, now known to be Ala⁴⁵ to Arg⁵⁸ (8). Not only had the minor peak been detected in the trypsin-modified EF-Tu-GDP preparations used for the crystallographic study described below, but the sequences of the NH₂-terminal fragments were determined (9). Sequencing was carried out on a Beckman 890M with the use of a 0.1M Quadrol program and

2.0 mg of Polybrene as a carrier (10). The major NH₂-terminal fragment was identified as Gly-Ile-Thr-Ile-Asn and corresponds to residues 59 to 63 in the EF-Tu sequence. Less than 10 percent of the material contained a second NH₂-terminal fragment, Leu-Leu-Asp-Glu, which corresponds to residues 264 to 267. As was expected, the acetylated NH₂-terminus of the protein was not detected by this method. However, an NH₂-terminal fragment, previously shown to correspond to residues 1 to 44 was detected by a sodium dodecyl sulfate (SDS) gel electrophoretic analysis (11). The NH₂-terminus of the 14-amino-acid fragment, residues 45 to 58, produced by the trypsin digestion, was not detected by any method in the material that was used for crystallization. Therefore, the findings indicate that the trypsin-modified EF-Tu used in the x-ray diffraction analysis described below contained only two major fragments corresponding to residues 1 to 44 and 59 to 393. A small portion of the latter fragment also contained a cleavage site at Lys²⁶³. Activity assays demonstrated that the trypsin-modified protein was fully active toward GDP and GTP exchange.

The trypsin-modified EF-Tu-GDP was crystallized by vapor diffusion techniques, with the parameters described previously (6). Two heavy atom derivatives were identified, the sites were located and refined by conventional methods, and the structure was solved at 5 Å resolution in the space group *P*₄₂₁₂ as reported previously (7). As a result of a space group transformation promoted by contaminants in the polyethylene glycol

F. Journak is an assistant professor in the Department of Biochemistry, University of California, Riverside 92521.

used in crystallization (12), the high resolution x-ray diffraction data were collected in the space group $C222_1$ with cell dimensions of $a = 98.609 \text{ \AA}$, $b = 100.807 \text{ \AA}$, $c = 162.465 \text{ \AA}$ and two molecules per asymmetric unit. The heavy atom reagents used in the preparation of isomorphous derivatives were dibromodiaminoplatinate and methyl mercury acetate. Crystals were transferred to mother liquor, which was subsequently adjusted to 0.1 mg/ml with the Pt compound or 2 mM with the Hg derivative, and soaked for 30 hours before the data were collected. All x-ray diffraction data, including Friedel pairs, were collected with the Mark II two-dimensional position-sensitive detector (13, 14). Each complete data set was recorded in 2 to 3 days from a single crystal; typically 90,000 reflections were measured to give 37,000 unique reflections to 2.7 Å resolution. The agreement factor, R , among symmetry-related and multiply-recorded reflections is given by $(\sum |I_{i,h} - \langle I_h \rangle|) / \langle I_h \rangle$ where $I_{i,h}$ is the intensity of the i th observation of reflection h . The R value ranged between 0.04 and 0.07 for each data set.

The heavy atom sites of each derivative were located independently by difference Patterson methods and were validated by cross-Fourier syntheses. The absolute configuration of each heavy atom constellation was determined by utilizing the intensity differences between Friedel pairs of reflections in the calculations (15). In all, there are six heavy atom sites for each derivative, two sets of three related by a pseudo 4₃ symmetry axis. The occupancy and coordinates of the six Pt and six Hg sites were refined by minimizing the differences between the calculated and the observed origin-removed Patterson according to the program written by Terwilliger (16). This method assumes a stringent error estimate for noncentric reflections which broadens the probability distribution and uniformly yields a lower figure of merit (FOM) in all cases tested (Tables 1 and 2). The multiple isomorphous replacement (MIR) phases calculated for the refined heavy atom positions including the anomalous dispersion component, were applied to the native structure amplitudes greater than three sigma, and an electron density map was calculated at 2.7 Å. To accentuate the structural features of the map, additional phasing information was derived from the automatic boundary determination and solvent flattening procedure of Wang (17), combined with the original MIR phases and applied to the calculation of a second electron density map at

2.7 Å. The parameters and results of the iterative Wang procedure are given in Table 3. Both electron density maps revealed similar information about the high resolution protein structure but the latter map, which included phasing information from the Wang procedure, was visually easier to interpret and therefore, was used in the subsequent analysis.

the ambiguities, additional phasing information from new derivatives and from the partial structural model must be incorporated into the electron density map before the assignment of all amino acids by computer graphic techniques is completed.

It is apparent from the 2.7 Å resolution electron density map that the trypsin-

Abstract. A 2.7 angstrom resolution x-ray diffraction analysis of a trypsin-modified form of the Escherichia coli elongation factor Tu reveals that the GDP-binding domain has a structure similar to that of other nucleotide-binding proteins. The GDP ligand is located at the COOH-terminal end of the β sheet and is linked to the protein via a Mg^{2+} ion salt bridge. The location of the guanine ring is unusual; the purine ring is located on the outer edge of the domain, not deep within a hydrophobic pocket. The amino acids from Pro¹⁰ to Arg⁴⁴ and from Gly⁵⁹ to Glu¹⁹⁰ have been assigned to the electron density with computer graphic techniques, and the resulting model is consistent with all known biochemical data. An analysis of the structure reveals that four regions of the amino acid sequence that are homologous with the family of ras oncogene proteins, termed p21, are located in the vicinity of the GDP-binding site, and most of the invariant amino acids shared by the proteins interact directly with the GDP ligand.

The polypeptide backbone was initially traced from the 2.7 Å resolution electron density maps stacked on plexiglass. Most of the α -carbon positions and amino acid residues are clearly visible in the map. Further confirmation of the correct tracing of the NH₂-terminal domain was derived from the positioning of two Hg atoms at Cys⁸¹ and Cys¹³⁷ and two Pt atoms at Met¹³⁹ and Met¹⁵¹, respectively. The amino acid sequence from residues 10 to 190 were subsequently fitted to the electron density by means of computer graphic techniques (18). In a region adjacent to residues 10 and 190 the electron density corresponding to approximately 25 residues is less well ordered, making a definitive interpretation difficult. The correct amino acid assignment in this region is particularly important for determining the direction of the interdomain polypeptide. Therefore, to resolve

modified EF-Tu-GDP is structured into three distinct domains. The most prominent and clearly defined domain is that of a six-stranded β sheet surrounded by six helices. The presence of both helical and β -strand secondary structural topology, as well as the location of the two major Hg sites, is consistent with all biochemical evidence identifying this domain as the NH₂-terminal portion of the protein. In addition, the prominence of the three highest peaks at one edge of the β sheet in this domain is suggestive of the GDP ligand site. A second domain, which is clearly visible in the electron density map, is that of a six-stranded, antiparallel β sheet. An additional β strand is wrapped around one side of the β sheet, forming a long, but narrow hydrophobic pocket. A tentative fit of the amino acid residues from 297 through 393 and the location of a Pt site at Met³⁴⁹ suggests

Table 1. Refined heavy atom-derivative parameters.

Compound	Occupancy	Atomic coordinates			
		X	Y	Z	B
Hg	0.558	0.6499	0.4376	0.0434	37.69
	0.565	0.9353	0.3468	0.2936	32.67
	0.466	0.7973	0.2213	0.0256	75.66
	0.464	0.7811	0.3007	0.7745	81.23
	0.069	0.5223	0.2166	0.1702	1.92
	0.225	0.7695	0.0180	0.9223	61.72
Pt	0.901	0.2406	0.4120	0.6643	76.08
	0.903	0.4064	0.2595	0.9103	64.99
	0.636	0.2319	0.2668	0.6011	66.75
	0.610	0.2591	0.2689	0.8491	75.66
	0.763	0.3713	0.2079	0.9871	142.09
	1.119	0.3073	0.3669	0.7464	264.25

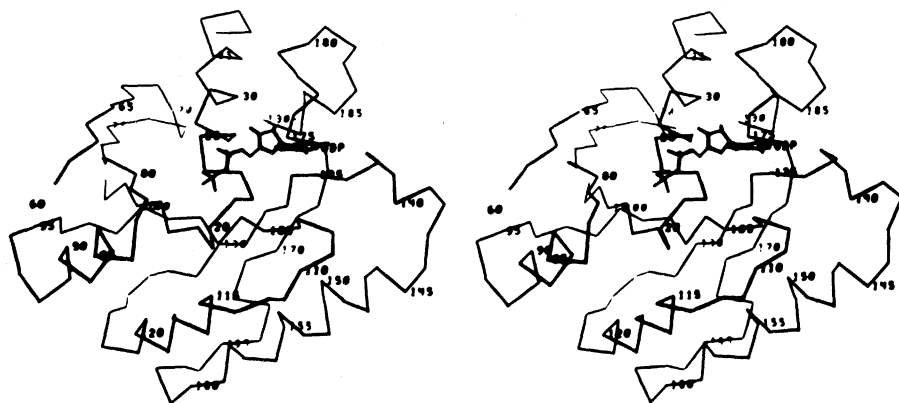


Fig. 1. Stereodigram of the unreduced α -carbon coordinates of the GDP-binding domain of trypsin-modified EF-Tu-GDP. Amino acid fragments from 10 to 44 and 59 to 190 are included in the figure with an identification label on every fifth amino acid.

that this domain represents the COOH-terminal region of the protein. The third domain clearly has the topology of a small β barrel, with a hydrophobic core extending 12 Å in diameter. A minor Hg site within the core region has been tentatively assigned to Cys²⁵⁵ and is consistent with the other structural results that this domain represents the intermediate polypeptide region extending approximately from amino acids 200 through 296. The domain appears to be somewhat flexible as the conformation of the β barrel differs for each of the

two molecules in the asymmetric unit.

As a result of ambiguities created by a flexible or possibly disordered polypeptide backbone in an interdomain region, a presentation of the complete structure of trypsin-modified EF-Tu-GDP is not justified until all methods for clarifying the ambiguities have been explored. However, the inclusion of additional phasing information may not necessarily resolve the ambiguities because such conformational flexibility in interdomain regions as well as in nucleic acid binding proteins are common and possibly rele-

vant to the function of the protein (19). Unlike the flexible region, the peptide backbone of the GDP-binding domain is very well ordered and the amino acid residues are clear. Moreover, the placement of the sequence into the electron density by computer graphic techniques is consistent with secondary structural predictions (20) as well as all known biochemical data for the domain residues. Therefore, I am presenting herein the structural results of only the GDP-binding domain of trypsin-modified EF-Tu. Because of amino acid homologies with other GDP-binding proteins (4), the structural identification of the amino acids in the NH₂-terminal domain of EF-Tu-GDP may be useful in designing site-directed mutagenesis experiments to localize the similar and dissimilar functions of other GDP-binding proteins.

A stereodigram of the unreduced α -carbon coordinates of the GDP-binding domain of the trypsin-modified EF-Tu-GDP is shown in Fig. 1 (21) and a schematic of the polypeptide backbone with approximately the same view is shown in Fig. 2. The first nine residues of the NH₂-terminus are located at one end of the β sheet in the region of the electron density that is ill defined. Therefore, the assignment of amino acids begins with Pro¹⁰, which is clearly visible in the map.

Table 2. Heavy atom derivative statistics.

Atom	Parameter	Average reflection range (Å)								
		10.0	6.3	5.0	4.2	3.7	3.4	3.1	2.8	Total
Hg	RMS(f)/RMS(E)*	2.05	2.41	1.32	1.07	1.02	0.91	1.04	0.91	1.31
	Centric R†	0.51	0.48	0.62	0.69	0.59	0.65	0.64	0.72	0.59
Pt	RMS(f)/RMS(E)	1.71	1.68	0.82	0.64	0.58	0.49	0.44	0.41	0.95
	Centric R	0.54	0.60	0.73	0.71	0.79	0.72	0.79	0.79	0.68
	Number of reflections: ($ F > 3\sigma$)	697	1261	1745	1973	2048	2085	1992	1685	13,486
	Mean figure of merit	0.77	0.62	0.54	0.41	0.44	0.45	0.36	0.34	0.53

*RMS(f) is the root-mean-square calculated heavy atom structure factor and RMS(E) is the root-mean-square lack of closure, given for the noncentric reflections only. †Centric $R = \sum_{hkl} (\Delta F_{hkl} - f_{hkl}) / N$.

Table 3. Automatic boundary determination and solvent flattening statistics for last of three cycles. (i) Fourier transform, (ii) molecular envelope and solvent mask, (iii) direct space filter assuming 35 percent solvent, (iv) Fourier inversion, and (v) reciprocal space filter. FOM, figure of merit.

Cycle	Average FOM	R* value	Average accumulated phase shift	Correlation coefficient†	Total				
1	0.56	0.47	38.0	0.85					
2	0.69	0.32	43.5	0.93					
3	0.75	0.26	46.2	0.95					
4	0.78	0.24	47.7	0.96					
5	0.79	0.22	48.8	0.97					
6	0.80	0.21	49.6	0.97					
7	0.80	0.20	50.2	0.97					
8	0.81	0.20	50.7	0.97					
Last cycle									
Resolution range (Å):	40.00	6.28	4.36	3.68	3.29	3.03	2.83	2.68	
Reflections (No.):	1755	3454	3292	2956	2772	2482	1886		18597
R value:	0.208	0.182	0.186	0.201	0.212	0.235	0.246		0.206

*R value = $[\sum_{hkl} (F_c - F_o)^2 / (F_o^2)]^{1/2}$ where F_c is the calculated structure factor amplitude from the Fourier inversion and F_o is the observed structure factor amplitude. †Correlation coefficient = $(F_c F_o) / [(F_o^2)(F_c^2)]^{1/2}$

The first β strand, located in the middle of the β sheet, begins with Val¹² and continues to His¹⁹. The next five residues form an unusual loop structure, which serves as a small binding pocket for the two phosphates of the GDP ligand. With Lys²⁴ as the beginning, the next 17 residues are coiled into a very long and regular α helix, which bisects one side of the β sheet and participates in the formation of two long hydrophobic pockets. The helix terminates at Gly⁴⁰, near to Arg⁴⁴, the first trypsin cleavage site. The next 14 amino acids, as shown by biochemical analysis, are not present in the C222₁ crystal form. The polypeptide tracing begins again at Gly⁵⁹ and forms β strand 2 at the edge of the sheet. This β strand, which is antiparallel to the others in the sheet, terminates in a short hairpin loop centered on Pro⁷². The next ten residues comprise the third β strand, from Thr⁷³ to Pro⁸² and then abruptly turn into a short helix from Gly⁸³ to Thr⁹³. After an extended crossover connection from Gly⁹⁴ to Met⁹⁸, the polypeptide backbone forms a typical mononucleotide fold of three parallel β strands from Asp⁹⁹ to Ala¹⁰⁶, Pro¹²⁸ to Leu¹³⁴, and Ile¹⁶⁹ to Gly¹⁷², respectively. Each adjacent β strand is connected to its neighbor by a helix. The 3₁₀ helix, from Glu¹¹⁴ to Gly¹²⁵, and the α helix from Glu¹⁴⁴ to Ser¹⁵⁸, are approximately parallel to one another and lie on the same side of the β sheet. After the sixth β strand, the polypeptide backbone forms a short 3₁₀ helix, from Ala¹⁷⁴ to Gly¹⁸⁰, a turn and then another helix which lies along one edge of the β sheet. After two turns ending at Glu¹⁹⁰, there appears to be a break in the helix and the backbone could branch in one of two directions. Because the electron density is not well ordered in this region, it is not possible to assign the amino acids residues at this stage to resolve the dual ambiguity.

The GDP ligand site is located at the COOH-terminal ends of β strands 1, 3, 4, and 5 (Fig. 2). A sample of the electron density map in the region of the GDP ligand is shown in Fig. 3. This ligand is linked to the protein via a Mg²⁺ ion, which forms a salt bridge with the Asp⁸⁰ side chain. The Mg²⁺ ion is located approximately 1.5 Å closer to the β -phosphate group and is consistent with results of electron paramagnetic and nuclear magnetic resonance (EPR and NMR) (22). The phosphates are nestled on the outside of a loop that joins the COOH-terminus of β strand 1 to the NH₂-terminus of α helix A. The location of the phosphates at the NH₂-terminus of an α helix is very common in nucleotide binding proteins, and it has been postulated

(23) that the positive dipole moment at the NH₂-terminus of an α helix partially neutralizes the negative charge on the phosphates. Also present at the NH₂-terminus of the helix is Lys²⁴ whose side chain appears to contribute to the charge neutralization of one phosphate group. Adjacent to the phosphates is the ribose ring in a C-2' *endo* conformation. One side of the ribose moiety is exposed to a solvent region.

The guanine ring is situated between the COOH-terminal end of the fourth β strand and the connecting loop of the β strand 5 and α helix D. The guanine ring

is in an *anti* conformation with respect to the sugar, but its location and orientation is surprising. The purine ring lies on the edge of the domain with the amino substituent on position 2 oriented away from the major portion of the protein (Fig. 3). The amino substituent, however, does appear to form a weak interaction with the side chain of Asp¹³⁸ on a protruding flexible loop of the protein. Although the protein has a high specificity for a guanine nucleotide, the only other distinguishing group is that of the oxygen substituent on position 6 of the ring which appears to lie in a small pocket

Fig. 2. Stylized schematic of the GDP-binding domain of trypsin-modified EF-Tu-GDP. Arrows represent β strands; cylinders, helices; and labeled open circles, the GDP ligand. The approximate location of the α carbons of selected amino acids is also shown.

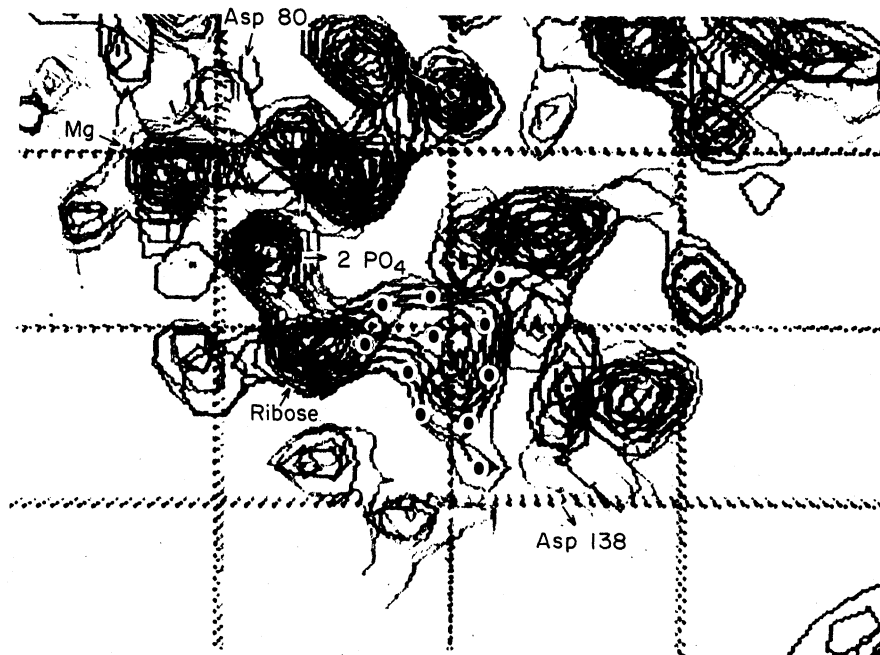
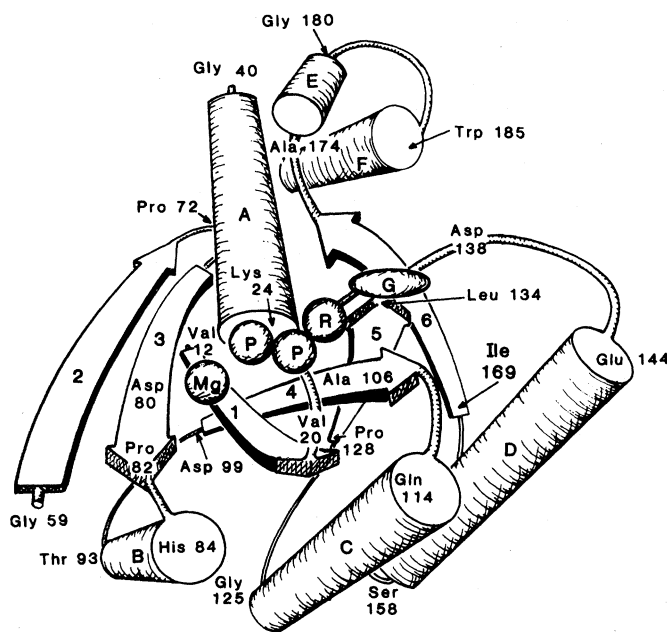


Fig. 3. A sample of the electron density in the region of the GDP ligand of trypsin-modified EF-Tu-GDP at 2.7 Å resolution. The atoms of the guanine ring are represented by closed black circles and the remaining groups of the GDP ligand are indicated by labels.

possibly interacting with several backbone amide groups. Moreover, the guanine ring is not buried in a deep hydrophobic pocket, contrary to the structural results of other nucleotide ligands. Several hydrophobic residues, including Ala¹⁰⁷, Phe¹³³, and Leu¹³⁴, do create a small pocket on one side of the guanine ring. In addition, the side chain of Asn¹³⁵ is located directly over the plane of the guanine ring, possibly forming several interactions with it.

Comparisons of the amino acid sequence of EF-Tu with other GDP-binding proteins, including the H-ras p21 protein, have revealed multiple homologous regions as well as several invariant amino acids. If conservative substitutions are permitted, there are four principal regions of shared sequence similarities, interspersed among stretches of nonaligned amino acids (4). In EF-Tu-GDP, the similar sequences include residues 15 to 29 for region 1, residues 79 to 87 for region 2, residues 99 to 108 for region 3, and residues 128 to 140 for region 4. The amino acids of region 1 exhibit the strongest homology and are located at the COOH-terminal end of β strand 1, the loop surrounding the two phosphate groups of the GDP ligand and the first turn of the α helix A. The residues of the second homologous region are found at the Mg²⁺ ion binding site, that is, the COOH-terminal end of the β strand 3 and the first turn of the adjacent α helix B. Regions 3 and 4 represent the β strand 4 and the connecting loop between β strand 5 and α helix D, respectively. Both regions are positioned around one side of the guanine ring and contribute side chains which may interact directly with it. Thus, all four principal regions of sequence homologies are located in the vicinity of the GDP-binding site. Those regions that do not share similar sequences are located at the NH₂-terminal end of the β sheet or in connecting polypeptide strands distant from the GDP ligand.

There are several invariant amino acids in all GDP binding proteins that have been sequenced (4). Most of the invariant amino acids form a direct contact with the GDP ligand in the EF-Tu structure. Asp⁸⁰ forms a salt bridge to the Mg²⁺ ion, Lys²⁴ partially neutralizes the charge on one phosphate group, Asn¹³⁵ is situated directly over the guanine ring, and Asp¹³⁸ interacts with the amino substituent of the guanine ring. Another amino acid of interest is Val²⁰ in EF-Tu which corresponds to Gly¹² in the H-ras p21 protein. The latter amino acid is considered critical for the activation of the transforming potential of the H-ras

protein (24). In EF-Tu, Val²⁰ is located on the outer edge of the loop which serves to position the phosphate groups of the GDP ligand at the junction of β strand 1 and α helix A. This location is consistent with the findings that complexation of H-ras p21 protein with monoclonal antibodies to the Gly¹² regions prevents the binding of the GTP ligand in the H-ras protein (25). The side chain of Val²⁰ in EF-Tu does not appear to interact directly with either phosphate, but it may be important for maintaining the proper backbone conformation of the loop. It is not difficult to imagine that a single amino acid substitution from glycine to valine or vice versa at this position would alter the backbone conformation and subsequently affect the phosphate binding site.

Different models for the GDP-binding domain of a protease-modified EF-Tu in space group C222₁ have been proposed (26, 27). The most recent Clark model agrees reasonably with the one presented herein, but only in the backbone assignment of Gly⁵⁹ through Glu¹⁹⁰. The two structural models are widely divergent in the assignment of Pro¹⁰ to Arg⁴⁴. In my model, this sequence is an integral part of the NH₂-terminal domain and the GDP-binding site, comprising β strand 1, the connecting loop, and α helix A. In the Clark model, this peptide fragment is assigned to electron density in the COOH-terminal domain and is approximately 25 Å distant from the GDP-binding site. This latter location is not compatible with the sequence homologies found in all GDP-binding proteins or with the recent studies of antibody complex formation on the H-ras p21 protein (25). Moreover, the placement of the amino acid residues into the electron density region proposed by Clark and co-workers does not result in a satisfactory fit when the 2.7 Å electron density map described above is used. Another inconsistency in the Clark model is the assignment of Ala⁴⁵ to Arg⁵⁸ to a distinctive strand of density located between two domains (27). Although this particular density is present in the C222₁ map described in this article, it cannot be assigned to the amino acids from 45 to 58 because the biochemical analysis clearly shows that this peptide fragment is missing in this crystal form. Given the difficulty of any high resolution structural analysis, minor errors in the polypeptide tracing are not uncommon. Nevertheless, the final structure must be compatible with the crystallographic data as well as all known biochemical data. The structural model of the GDP-binding domain of trypsin-modified EF-Tu present-

ed above fulfills these criteria and provides a plausible model with which to design experiments for the H-ras oncogene protein and other GDP-binding proteins.

References and Notes

1. D. L. Miller and H. Weissbach, in *Molecular Mechanisms of Protein Biosynthesis*, S. Pestka and H. Weissbach, Eds. (Academic Press, New York, 1977), p. 323.
2. E. M. Scolnick, A. G. Papageorge, T. Y. Shih, *Proc. Natl. Acad. Sci. U.S.A.* **76**, 5355 (1979).
3. R. Leberman and U. Egner, *EMBO J.* **3**, 339 (1984).
4. K. Halliday, *J. Cyclic Nucleotide Prot. Phosphoryl. Res.* **9**, 435 (1984).
5. M. A. Lochrie, J. B. Hurley, M. I. Simon, *Science* **228**, 96 (1985).
6. F. Journak, D. Miller, A. Rich, *J. Mol. Biol.* **115**, 103 (1977).
7. F. Journak, A. McPherson, A. Wang, A. Rich, *J. Biol. Chem.* **255**, 6751 (1980).
8. K. Arai *et al.*, *Proc. Natl. Acad. Sci. U.S.A.* **77**, 1326 (1980).
9. Sequencing was performed by the Protein Structure Laboratory, University of California, Davis.
10. S. B. Smith, J. W. Richards, W. F. Benisek, *J. Biol. Chem.* **255**, 2678 (1980).
11. A. Wittinghoffer, R. Frank, R. Leberman, *Eur. J. Biochem.* **108**, 423 (1980).
12. F. Journak, *J. Mol. Biol.*, in press.
13. Data were collected at the Multiwire Area Detector Resource Facility at the University of California, San Diego, courtesy of Drs. N. Xuong and R. Hamlin.
14. R. Hamlin *et al.*, *J. Appl. Cryst.* **14**, 85 (1981).
15. T. L. Blundell and L. Johnson, *Protein Crystallography* (Academic Press, London, 1977), p. 373.
16. T. Terwilliger and D. Eisenberg, *Acta Cryst.* **A39**, 813 (1983).
17. B. C. Wang, *ibid.* **A40**, C12 (1984).
18. GRIP-75 molecular graphics system built by Computer Graphics Resource Facility, University of North Carolina. Major contributions to GRIP-75 have been made by E. G. Britton, J. S. Lipscomb, M. E. Pique, D. Tolle, and W. E. Siddall, under the direction of W. V. Wright, and by J. E. McQueen, Jr., under the direction of J. Hermans.
19. T. N. Bhat and D. M. Blow, *Acta Cryst.* **A38**, 22 (1982).
20. R. A. Laursen, S. Nagarkatti, D. L. Miller, *FEBS Lett.* **80**, 103 (1977).
21. The atomic coordinates of trypsin-modified EF-Tu-GDP will be deposited in the Brookhaven Protein Data Bank upon completion of the structural refinement process.
22. A. Wittinghoffer, R. S. Goody, P. Roesch, H. R. Kalbitzer, *Eur. J. Biochem.* **124**, 109 (1982).
23. W. G. J. Hol, P. T. van Duijnen, H. J. C. Berendsen, *Nature (London)* **273**, 443 (1978).
24. C. Tabin *et al.*, *ibid.* **300**, 143 (1982).
25. R. Clark, G. Wong, N. Arnheim, D. Nitelki, F. McCormick, *Proc. Natl. Acad. Sci. U.S.A.*, **82**, 5280 (1985).
26. K. Morikawa, T. F. M. LaCour, J. Nyborg, K. M. Rasmussen, D. L. Miller, B. F. C. Clark, *J. Mol. Biol.* **125**, 325 (1978).
27. B. F. C. Clark, in *Cell Function and Differentiation* (Liss, New York, 1982), part C, pp. 59-64.
28. The structural analysis of a protein is a major undertaking that involves contributions from many individuals. I thank the following people without whose assistance the research would not yet have been completed: N. G. Xuong and R. Hamlin for use of the multiwire area detector facility at the University of California, San Diego; A. McPherson and members of his laboratory, including D. Cascio, R. Williams, R. Morrison, and G. DeLozier at the University of California, Riverside, for making their crystallographic computer software available to me; B. C. Wang of the University of Pittsburgh for making his computer program available to me; F. P. Brooks, Jr., M. Pique, and members of the computer graphics resource facility at the University of North Carolina for use of the GRINCH and GRIP systems; A. Olson of the Research Institute of Scripps Clinic for computer graphics assistance with Fig. 1; F. McCormick of Cetus Corporation for communicating data prior to publication; the UCR Academic Computer Center for partial computer support and the United States Public Health Service for financial support (GM 26895).

12 June 1985; accepted 20 August 1985